

AMCoR

Asahikawa Medical University Repository <http://amcor.asahikawa-med.ac.jp/>

Stem cells translational medicine. (2016.8) 5(8):1067–78.

Apoptosis-Resistant Cardiac Progenitor Cells Modified With Apurinic/Apyrimidinic Endonuclease/Redox Factor 1 Gene Overexpression Regulate Cardiac Repair After Myocardial Infarction.

Aonuma T, Takehara N, Maruyama K, Kabara M, Matsuki M, Yamauchi A, Kawabe J, Hasebe N.



Apoptosis-Resistant Cardiac Progenitor Cells Modified With Apurinic/Apyrimidinic Endonuclease/Redox Factor 1 Gene Overexpression Regulate Cardiac Repair After Myocardial Infarction

TATSUYA AONUMA,^a NAOFUMI TAKEHARA,^{a,b} KEISUKE MARUYAMA,^a MAKI KABARA,^{a,b} MOTOKI MATSUKI,^a ATSUSHI YAMAUCHI,^a JUN-ICHI KAWABE,^{a,b} NAOYUKI HASEBE^a

Key Words. Apoptosis • Sca-1 • Gene expression • Cellular therapy • Stem/progenitor cell

^aDivision of Cardiology, Nephrology, Pulmonology, and Neurology, Department of Internal Medicine, and ^bDepartment of Cardiovascular Regeneration and Innovation, Asahikawa Medical University, Asahikawa, Japan

Correspondence: Naofumi Takehara, M.D., Ph.D., 2-1-1-1 Midorigaoka-higashi, Asahikawa, 078-8510, Japan. Telephone: 81-166-68-2442; E-Mail: takenao1@mac.com

Received October 12, 2015; accepted for publication March 14, 2016; published Online First on June 22, 2016.

©AlphaMed Press
1066-5099/2016/\$20.00/0

<http://dx.doi.org/10.5966/sctm.2015-0281>

ABSTRACT

Overcoming the insufficient survival of cell grafts is an essential objective in cell-based therapy. Apurinic/aprimidinic endonuclease/redox factor 1 (APE1) promotes cell survival and may enhance the therapeutic effect of engrafted cells. The aim of this study is to determine whether APE1 overexpression in cardiac progenitor cells (CPCs) could ameliorate the efficiency of cell-based therapy. CPCs isolated from 8- to 10-week-old C57BL/6 mouse hearts were infected with retrovirus harboring APE1-DsRed (APE1-CPC) or a DsRed control (control-CPC). Oxidative stress-induced apoptosis was then assessed in APE1-CPCs, control-CPCs, and neonatal rat ventricular myocytes (NRVMs) cocultured with these CPCs. This analysis revealed that APE1 overexpression inhibited CPC apoptosis with activation of transforming growth factor β -activated kinase 1 (TAK1) and nuclear factor (NF)- κ B. In the coculture model, NRVM apoptosis was inhibited to a greater extent in the presence of APE1-CPCs compared with control-CPCs. Moreover, the number of surviving DsRed-positive CPC grafts was significantly higher 7 days after the transplant of APE1-CPCs into a mouse myocardial infarction model, and the left ventricular ejection fraction showed greater improvement with attenuation of fibrosis 28 days after the transplant of APE1-CPCs compared with control-CPCs. Additionally, fewer inflammatory macrophages and a higher percentage of cardiac α -sarcomeric actinin-positive CPC-grafts were observed in mice injected with APE1-CPCs compared with control-CPCs after 7 days. In conclusion, antiapoptotic APE1-CPC graft, which increased TAK1-NF- κ B pathway activation, survived effectively in the ischemic heart, restored cardiac function, and reduced cardiac inflammation and fibrosis. APE1 overexpression in CPCs may serve as a novel strategy to improve cardiac cell therapy. STEM CELLS TRANSLATIONAL MEDICINE 2016;5:1067–1078

SIGNIFICANCE

Improving the survival of cell grafts is essential to maximize the efficacy of cell therapy. The authors investigated the role of APE1 in CPCs under ischemic conditions and evaluated the therapeutic efficacy of transplanted APE1-overexpressing CPCs in a mouse model of myocardial infarction. APE1 hindered apoptosis in CPC grafts subjected to oxidative stress caused in part by increased TAK1-NF- κ B pathway activation. Furthermore, APE1-CPC grafts that effectively survived in the ischemic heart restored cardiac function and attenuated fibrosis through pleiotropic mechanisms that remain to be characterized. These findings suggest that APE1 overexpression in CPCs may be a novel strategy to reinforce cardiac cell therapy.

INTRODUCTION

Regenerative therapy for cardiovascular disease represents hope for hundreds of millions of patients [1]. Cell-based therapy has been attempted using various somatic cell types, including bone marrow [2, 3], endothelial progenitor cells [4], skeletal myoblasts [5], mesenchymal stem cells [6], and cardiac progenitor cells (CPCs) derived from the postnatal heart, which can be readily

differentiated into cardiomyocytes [7]. Actually, this form of therapy has been a partial success in completely curing severe heart failure or ischemic cardiomyopathy [8, 9]. However, in cardiac cell therapy, oxidative stress-induced reactive oxygen species (ROS) affect not only host organs, but also grafted tissues in ischemic heart disease. As such, most radiolabeled or magnetic-labeled cell grafts are lost within 4 weeks of transplantation because of their inability to withstand

oxidative stress in the ischemic myocardium [10, 11]. We have also reported that poor graft survival was observed after direct injection into ischemic porcine heart in cardiac magnetic resonance imaging [12]. Thus, improving the survival of cell grafts in host hearts is essential to maximize the efficacy of cardiac cell therapy.

Apurinic/apyrimidinic endonuclease/redox factor 1 (APE1) is known as a multifunctional enzyme [13, 14] that activates the DNA repair pathway (endonuclease) and induces redox-sensitive transcription factors such as activator protein 1, p53, hypoxia-inducible factor-1 α , and nuclear factor (NF)- κ B, to encourage cell survival and differentiation [15–18]. Endonuclease sites activate base excision repair (BER) enzymes that remove the damaged base of DNA in the various cell types [19]. Alternatively, highly stressful oxidative environments such as atherosclerotic plaques [20] and the central nervous system (e.g., cerebral ischemia, degenerative diseases) [21] induce the upregulation of the redox factor 1 (Ref-1) site, which acts as a redox system in damaged organs. We recently reported that APE1 enhanced vascular repair *in vivo* by promoting endothelial progenitor cell adhesion in an APE1 redox-dependent manner [22]. As such, clarifying the activities of APE1, as well as their underlying mechanisms, may reveal potential approaches to improving graft cell survival and function in cell-based therapy.

The present study investigated the role of APE1 in CPCs under ischemic conditions. Furthermore, we also evaluated the therapeutic efficacy of transplanted APE1-overexpressing CPCs in mitigating the cardiac damage in a mouse model of myocardial infarction (MI).

MATERIALS AND METHODS

Materials and methods in detail are available in the supplemental online data.

Isolation and Culture of Stem Cell Antigen 1-Positive CPCs

Hearts from 8- to 10-week-old C57B/6 male mice were minced and treated twice with 0.2% type II collagenase and 0.01% DNase I (Worthington Biochemical Corp., Lakewood, NJ, <http://www.worthington-biochem.com>) for 20 minutes at 37°C. Isolated cells were size-fractionated with a 30%–70% Percoll gradient to obtain single-cell suspensions devoid of debris and fibrotic tissues. Purified cells were cultured in Dulbecco's modified Eagle's medium (DMEM)/F-12 (Thermo Fisher Scientific Life Sciences, Waltham, MA, <http://www.thermofisher.com>) supplemented with 10% fetal bovine serum, penicillin/streptomycin, and 40 ng/ml mouse recombinant basic fibroblast growth factor (bFGF) (R&D Systems, Minneapolis, MN, <http://www.rndsystems.com>) at 37°C and 5% CO₂. Expanded cells were incubated with stem cell antigen (Sca)-1 antibody-conjugated magnetic beads (Miltenyi Biotec, Bergisch Gladbach, Germany, <http://www.miltenyibiotec.com>) to obtain a pure population of Sca-1-positive CPCs by magnetic-activated cell sorting.

Retroviral Infection and Fluorescence-Activated Cell Sorting

pRetroX-IRES-DsRed Express Vectors (Clontech, Mountain View, CA, <http://www.clontech.com>) harboring a DsRed gene sequentially tagged with or without a human APE1 gene were prepared as described previously [22]. Recombinant plasmids were transfected into GP2-293 cells (Clontech) using Lipofectamine-LTX

(Thermo Fisher Scientific Life Sciences, Waltham, MA, <http://www.thermofisher.com>). After incubation for 48–60 hours, retroviral media was added to harvested CPCs along with polybrene (7 μ g/ml). Cells infected with the DsRed or APE1-DsRed vectors were expanded and sorted based on DsRed expression on a FACSAria II instrument (BD Biosciences, San Jose, CA, <http://www.bdbiosciences.com>). After cell sorting, CPCs with APE1-DsRed (APE1-CPC) or DsRed (control-CPC) expression were expanded for use in experiments.

Immunohistochemistry Analysis

Cells were washed in phosphate-buffered saline (PBS) for 10 minutes before fixing with 2% paraformaldehyde (PFA). Fixed samples were incubated in PBS containing 2% Block ACE (AbD Serotec, Kidlington, UK, <http://www.abdserotec.com>) for 1 hour and incubated with specific anti-APE1 primary antibody (Novus Biologicals, Littleton, CO, <http://www.novusbio.com>) at 4°C overnight, followed by staining with secondary antibodies conjugated to Alexa Fluor 488 (Thermo Fisher Scientific Life Sciences). Nuclei were counterstained with mounting medium containing Hoechst 33258 (Lonza, Portsmouth, NH, <http://www.lonza.com>). Images were collected by a fluorescence microscope (BZ-X710; Keyence, Osaka, Japan, <http://www.keyence.com>).

Reverse Transcription-Polymerase Chain Reaction

Total RNA was extracted from CPCs, control-CPCs, APE1-CPCs, cardiac-differentiated CPCs (as described in the supplemental online data), and heart samples (sham operation, control-medium injection, and cell injection) using the RNeasy Mini kit (Qiagen, Valencia, CA, <http://www.qiagen.com>) and reversed-transcribed into complementary DNA using SuperScript-III Reverse Transcriptase (Thermo Fisher Scientific Life Sciences). Reverse transcription-polymerase chain reaction (RT-PCR) for the semiquantitative analysis of mRNA expression was carried out using LA-Taq (TaKaRa Bio, Shiga, Japan, <http://www.takara-bio.com>) with primers specific for mouse and human *APE1*, mouse *Nanog*, mouse F-box-containing protein 15 (*Fbx15*), mouse myocyte enhancer factor 2c (*Mef2c*), mouse telomerase reverse transcriptase (*Tert*), mouse cardiac troponin I (*Tnl*), and mouse glyceraldehyde-3-phosphate dehydrogenase (*Gapdh*) (Invitrogen). Quantitative RT-PCR for mouse interleukin (IL)-1 β and IL-6 was performed using Taqman Gene Expression Master Mix (Applied Biosystems, Foster City, CA, <http://www.appliedbiosystems.com>) on a 7300 RT-PCR system (Applied Biosystems).

APE1 Gene Knockdown in CPCs by RNA Interference

CPCs were incubated until they reached 60%–80% confluence. ON-TARGET plus Mouse *Ape1* short interfering RNA (siRNA) (CPC^{siAPE1(+)}) or nontargeting siRNA (CPC^{siAPE1(-)}) (Dharmacon, Lafayette, CO, <http://dharmacon.gelifsciences.com/>) was transfected to CPCs using Lipofectamine RNAi-MAX Reagent (Life Technologies) according to the manufacturer's recommendations. The next day, the culture medium was replaced with DMEM/F12. Experiments were performed 60–72 hours after RNAi transfection.

H₂O₂-Induced ROS and Apoptosis Assay

CPCs, control-CPCs, and APE1-CPCs grown in 96-well cell culture plates were incubated with dichloro-dihydro-fluorescein

diacetate-containing medium (OxiSelect Intracellular ROS Assay kit; Cell Biolabs, San Diego, CA, <http://www.cellbiolabs.com>) at 37°C for 30 minutes in the dark. The medium was replaced with serum-free medium with or without 0.5 mmol/L hydrogen peroxide. The level of fluorescence was calculated with a Multiskan FC Microplate Photometer (Thermo Fisher Scientific Life Sciences) 3 hours after the exposure of hydrogen peroxide. For the terminal deoxynucleotidyl transferase dUTP nick-end labeling (TUNEL) assay, cells were fixed with 2% PFA for 10 minutes at room temperature. After permeabilization with PBS containing 0.1% Triton X-100 and 0.1% sodium citrate for 2 minutes at 4°C, cells were incubated with fluorescein isothiocyanate-conjugated TUNEL reaction mixture (In Situ Cell Death Detection kit; Roche Diagnostics, Indianapolis, IN, <http://usdiagnostics.roche.com/>) for 60 minutes at 37°C. Samples were stained with 4',6-diamidino-2-phenylindole to label nuclei and visualized under an epifluorescence microscope. TUNEL-positive cells were counted in at least six random microscopic fields under a 10× objective.

Western Blot Analysis

Control-CPCs, APE1-CPCs, CPCs^{siAPE1(+)}, and CPCs^{siAPE1(-)} were incubated with 50 ng/ml recombinant murine tumor necrosis factor (TNF)- α (PeproTech, Rocky Hill, NJ, <http://www.peprotech.com>) for the indicated times, and total cellular protein was extracted using an NP40 cell lysis buffer (Thermo Fisher Scientific Life Sciences) mixed with cComplete and PhosStop inhibitors (both from Roche Diagnostics). After blocking with 5% skim milk, the membranes were incubated overnight with primary antibodies at 4°C, followed by horseradish peroxidase-conjugated secondary antibodies at room temperature. Primary antibodies were as follows: rabbit monoclonal antibody against NF- κ B, phospho-NF- κ B, transforming growth factor β -activated kinase (TAK)1, and β -actin (all from Cell Signaling Technologies, Danvers, MA, <http://www.cellsignal.com>). Signals were visualized using an enhanced chemiluminescence system (LAS-3000; Fujifilm, Tokyo, Japan, <http://www.fujifilm.com>) and Multi-Gauge software (Fujifilm).

Enzyme-Linked Immunosorbent Assay

CPCs, control-CPCs, and APE1-CPCs grown in 96-well plates were incubated with 120 μ l of serum-free media with or without recombinant human NF- κ B p65 protein (Active Motif, Carlsbad, CA, <http://www.activemotif.com>). After incubation for 4 hours, the IL-6 concentration in each culture supernatant was determined using a Mouse IL-6 ELISA Kit (Thermo Fisher Scientific Life Sciences). The level of fluorescence was calculated with a Multiskan FC Microplate Photometer.

Coculture With Neonatal Rat Ventricular Myocytes Under Anoxic Conditions

Neonatal rat ventricular myocytes (NRVMs) were obtained from neonatal (1-day-old) rat hearts (supplemental online data). After NRVMs were at 50% confluence, APE1-CPCs were added at the ratios of 15:1, 6:1, 3:1, and 2:1, in varying concentrations of atmospheric oxygen, to determine the necessary conditions to best visualize NRVM apoptosis. According to these results, 5.0×10^4 cells of control-CPCs or APE1-CPCs were cocultured with 1.5×10^5 NRVMs (3:1 ratio) for future analyses. The next day, culture medium was replaced with serum-free medium and cells were cultured for 3 days in an anoxic environment using

AnearoPack-Anaero (Mitsubishi Gas Chemical Co., Tokyo, Japan, <http://www.mgc.co.jp>). Alternatively, cells were cultured in the presence of a selective functional antagonist of the APE1-redox domain E3330 (40 μ M) for 2 days in an anoxic environment. The TUNEL assay was performed as described above, followed by cardiac α -sarcomeric actinin (α -SA) labeling to detect NRVMs.

Mouse Model of MI

C57BL/6 mice were anesthetized and ventilated with 3% isoflurane after intubation. The left anterior coronary was occluded directly under the left atrium using monofilament nylon 8-0 sutures (Ethicon, Somerville, NJ, <http://www.ethicon.com>) for 45 minutes. After the occlusion was released, control-medium, 10^6 APE1-CPCs, or 10^6 control-CPCs suspended in 30 μ l PBS were injected at the three sites within the ischemic border zone of the left ventricle (LV).

Histologic Analysis

Hearts harvested from mice 7 and 28 days after the operation were fixed in PFA at 4°C, followed by treatment with sucrose solution. Heart sections 28 days after the operation were subjected to Masson's trichrome staining to evaluate fibrosis area using ImageJ software (NIH, Bethesda, MD, <http://imagej.nih.gov/ij>). Infarct size was calculated by measuring the fibrosis area as a percentage of the total LV area. Cardiomyocytes and blood vessels were stained with anticardiac α -SA antibody and anti-cluster of differentiation 31 (anti-CD31) antibodies, respectively, 7 days after the operation. The number of engrafted cells that differentiated into cardiac α -SA and DsRed double-positive cardiomyocytes and the number of CD31-positive blood vessels were counted in at least four high-power microscopic fields ($\times 20$) each for infarct and border zones 7 days after the operation. Macrophages were identified by labeling with anti-CD68, anti-CD86, and anti-CD206 antibodies, and the numbers of M1 macrophages (CD68⁺CD206⁻ or CD86⁺) and M2 macrophages (CD206⁺) were counted in at least 10 high-power microscopic fields ($\times 20$) 7 days after the operation.

Statistical Analysis

Experimental data are presented as mean \pm SD. Sample number (n) is shown in the figure legends. The statistical significance of differences in vitro (qRT-PCR, ROS assay, TUNEL assay, Western blotting) was evaluated with the Student's t test. Nonparametric in vivo data (graft cell survival, LV ejection fraction [LVEF], fibrotic area, intramuscular cytokines, macrophages, and vessel count) were assessed by the Mann-Whitney U test. $p < .05$ was considered to be statistically significant. Data were analyzed using JMP9 (JMP, Tokyo, Japan, <http://www.jmp.com>).

RESULTS

Characterization of Sca1-CPCs and APE1-Overexpressing CPCs

Fluorescence-activated cell sorting (FACS) analysis showed that Sca-1⁺ sorted cells were positive for CD29, CD105, CD90, and vascular cell adhesion molecule 1 (also known as CD106), but negative for the hematopoietic markers CD31, CD45, and CD11b (supplemental online Fig. 1A). DsRed protein expression in transfected APE1-CPCs and control-CPCs was confirmed by immunochemistry (supplemental online Fig. 1B). In RT-PCR analysis,

human APE1 gene expression was found only in APE1-CPCs and was detectable until passage 11 (Fig. 1A; supplemental online Fig. 1C). Next, we evaluated cell surface antigen and transcription factor expression in both control-CPCs and APE1-CPCs to assess whether APE1 gene overexpression affected CPC phenotype; however, FACS and RT-PCR analysis showed no differences in the expression of cell surface antigens (positive for CD29, CD105, CD106, partial positive for CD90, and negative for CD31, CD45, CD11b) or transcriptional factors (*Nanog*, *Fbx15*, *Mef2c*, *Tert*) between control-CPCs and APE1-CPCs (Fig. 1B and 1C). To clarify the different function of APE1 protein in AP endonuclease (BER) pathway and Ref-1, we evaluated intracellular localization of APE1 protein in normal and anoxia culture conditions. In normal culture conditions, APE1 protein expression of both control-CPCs and APE1-CPCs was shown in subcellular localization rather than in nucleus (Fig. 1D1, D2). In anoxic conditions, the expression of APE1 protein of APE1-CPCs increased in subcellular localization without nuclear translocation (Fig. 1D6), but did not increase in control-CPCs compared with normal conditions (Fig. 1D5).

We also investigated the role of APE1 overexpression on cardiogenesis of CPCs. First, in NRVM coculture, we confirmed that DsRed-positive CPCs differentiated into cardiomyocytes with sarcomere (supplemental online Fig. 1D). Fourteen days after induction in CPC cardiogenesis assay without NRVM coculture, mRNA expression analysis in differentiated CPCs revealed significant increases in *Mef2c* and *Tnl* in both control-CPCs and APE1-CPCs. Differentiation-specific expression differences were not observed between the two groups (Fig. 1E).

APE1 Overexpression Inhibits H₂O₂-Induced ROS Production and Apoptosis in CPCs via TAK1/NF- κ B Pathway Activation

The effect of APE1 overexpression in CPCs under ischemic conditions was assessed in vitro by exposing the cells to H₂O₂. ROS levels in CPCs increased after 3 hours of H₂O₂ exposure, but were significantly lower in APE1-CPCs ($1,306 \pm 131 \mu\text{M}$) than in CPCs ($1,739 \pm 408 \mu\text{M}$) or control-CPCs ($1,735 \pm 259 \mu\text{M}$; $p < .05$) (Fig. 2A). TUNEL assays revealed that the ratio of apoptotic cells in control-CPCs increased ~23%–25% after 48 hours of H₂O₂ exposure. In contrast, the ratio of apoptotic cells in APE1-CPCs ($12.9\% \pm 9.5\%$) significantly decreased compared with that in CPCs ($22.9\% \pm 8.1\%$) and control-CPCs ($24.7\% \pm 11.7\%$; $p < .05$) (Fig. 2B; supplemental online Fig. 2A1–2A6). Conversely, RNAi-mediated APE1 knockdown increased the ratio of apoptotic APE1-CPCs after H₂O₂ treatment from $19.2\% \pm 8.0\%$ to $46.5\% \pm 14.9\%$ (Fig. 2C).

Next, we investigated whether the signaling pathways associated with apoptosis were differentially activated in control-CPCs and APE1-CPCs. According to results from a protein array analysis in cells subjected to H₂O₂ (supplemental online Table 1), we focused in the relationship between APE1 and TAK1 activation. Western blot analysis revealed that TNF- α -induced TAK1 activation was enhanced in APE1-CPCs compared with control-CPCs (1.5 ± 0.4 -fold vs. 3.0 ± 1.6 -fold; $p < .05$), which was accompanied by increased NF- κ B phosphorylation relative to controls (3.4 ± 0.6 -fold vs. 5.0 ± 0.6 -fold; $p < .05$) (Figs. 2D and 2E). Conversely, APE1 knockdown significantly interfered with the TNF- α -induced TAK1 activation and NF- κ B phosphorylation in CPCs (TAK1 activation: CPC^{siAPE1(-)}, 1.2 ± 0.2 -fold;

CPC^{siAPE1(+)}, 1.0 ± 0.2 -fold; $p < .05$; NF- κ B phosphorylation: CPC^{siAPE1(-)}, 2.4 ± 0.5 -fold; CPC^{siAPE1(+)}, 1.8 ± 0.2 -fold; $p < .01$) (Fig. 2F and 2G). To assess the relationship between the cellular stress response and NF- κ B activation, we evaluated inflammatory IL-6 secretion stimulated by NF- κ B exposure and/or nutrient deprivation by serum starvation. Under moderate nutritional deprivation-induced stress, APE1 overexpression inhibited IL-6 secretion by CPCs (control-CPCs, 124.6 ± 26.5 pg/ml; APE1-CPCs, 75.6 ± 39.8 pg/ml; $p < .05$). Conversely, exposure to 100 ng NF- κ B—acting as a nonphysiological ectopic stimulus—increased IL-6 secretion by both control-CPCs and APE1-CPCs (Fig. 2H).

Mode of Action of APE1-CPCs to Ex Vivo and In Vivo Ischemic Heart

To assess the antiapoptotic effect of APE1-CPCs, we performed TUNEL assays in CPC and NRVM cocultures after 3 days of anoxic conditions. NRVM apoptosis was inhibited by coculturing with CPCs, and the extent of this suppression was greater in the presence of APE1-CPCs compared with control-CPCs (Fig. 3A and 3B). Therefore, the number of surviving NRVMs was higher when cultured with APE1-CPCs compared with control-CPCs or control-medium (Fig. 3C). To clarify whether this beneficial effect of APE1 is based on redox function, we evaluated NRVM survival in coculture experiments with control-CPCs or APE1-CPCs in the presence of E3330, a selective functional antagonist of the APE1-redox domain. Notably, the inhibitory effect of APE1 overexpression on anoxia-induced apoptosis was markedly attenuated with E3330 exposure (Fig. 3B and 3C). Next, we assessed the survival of CPC grafts in the host heart 7 days after cell injection in a mouse MI model. The number of DsRed-positive CPC grafts was significantly higher in the APE1-CPC group than in the control-CPC group and was observed more in the border zone than the infarct zone (Fig. 3D and 3E).

Transplantation of APE1-Overexpressing CPCs Improves Cardiac Function and Cardiac Fibrosis After MI

We randomly assigned MI mice to groups for injection with control-medium, control-CPCs, or APE1-CPCs to evaluate the effect of cell-based therapy using APE1-CPCs on MI. Analysis of the absolute change in the LV ejection fraction (LVEF) using M-mode echocardiogram revealed deterioration in the control-medium group compared with baseline at 24 hours and 4 weeks after MI. However, LVEF in the two cell-injected groups was improved in comparison with the control-medium group from day 1 to day 28. Furthermore, the absolute change of LVEF in the APE1-CPC group ($11.2\% \pm 4.0\%$) was significantly greater than that of the control-CPC ($3.1\% \pm 6.7\%$; $p < .01$) and control-medium ($-3.5\% \pm 5.3\%$; $p < .01$) ($p < .05$ for control-medium vs. control-CPC) (Fig. 4A and 4B). The occurrence of cardiac fibrosis was evaluated by Masson's trichrome staining 4 weeks after MI to determine infarct size in the ischemic hearts (Fig. 4C). Cardiac fibrosis in the control-medium group was observed in >15% of LVs. In the control-CPC group, the size of cardiac fibrosis was smaller than in the control-medium group, but this was not statistically significant. However, cardiac fibrosis in the APE1-CPC group was significantly smaller than in the control-medium and control-CPC groups (control-CPC, $12.9\% \pm 6.2\%$; APE1-CPC, $6.8\% \pm 3.5\%$; $p < .05$) (Fig. 4D).

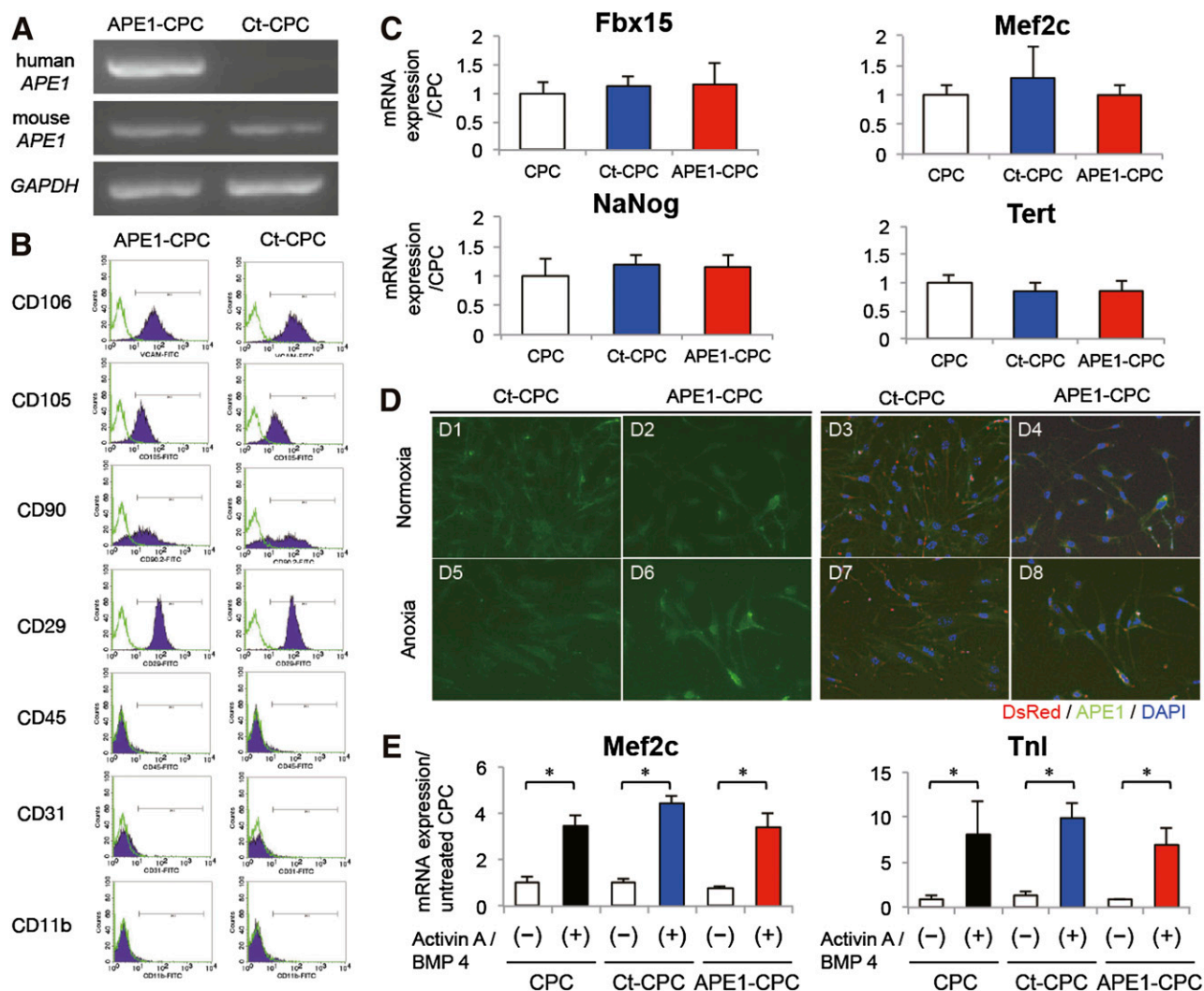


Figure 1. Characteristics of APE1-overexpressing CPCs. **(A):** Exogenous human APE1 levels as determined by RT-PCR; expression was detected in APE1-CPCs but not control-CPCs. There was no difference in the expression level of endogenous mouse-APE1 between the two cell lines. **(B):** Analysis of cell surface marker expression in control-CPCs and APE1-CPCs ($n = 3$, respectively). Both cells were positive for vascular cell adhesion molecule, CD106, CD 29, CD105, and CD90 and negative for CD31, CD45, and CD11b. **(C):** Quantitative RT-PCR analysis showed the mRNA expression of transcriptional genes. There was no difference in the expression level of mouse *Nanog* ($n = 10$); F-box-containing protein 15 (*Fbx15*; $n = 6$), myocyte enhancer factor 2c (*Mef2c*; $n = 6$), and telomerase reverse transcriptase (*Tert*; $n = 6$) between the three cell lines. **(D):** Intracellular localization of APE1-protein in normoxic and anoxic conditions ($n = 3$, respectively). Left: green, APE1; right: merged image of APE1 (green), DsRed (red), and cell nuclei (blue). Magnification $\times 40$. **(E):** Quantitative RT-PCR analysis showed the ratio of mRNA expression of cardiogenesis genes (*Mef2c*, troponin-I) compared with untreated CPCs in the three cell lines ($n = 4$, respectively). *, $p < .05$. Abbreviations: APE1, apurinic/apyrimidinic endonuclease/redox factor 1; BMP, bone morphogenetic protein; CD, cluster of differentiation; CPC, cardiac progenitor cell; Ct, control; DAPI, 4',6-diamidino-2-phenylindole; GAPDH, glyceraldehyde-3-phosphate dehydrogenase; RT-PCR, reverse transcription-polymerase chain reaction; Tnl, troponin I.

Cardiac Inflammation Is Attenuated by APE1-CPC Transplantation

To assess the pleiotropic effect of enhanced CPC graft survival, we investigated the inflammatory response in the host MI heart. Three days after operation, IL-6 expression in the ischemic heart tissue was attenuated in both control-CPC and APE1-CPC groups compared with the control-medium group. Furthermore, IL-1 β expression was significantly attenuated only in the APE1-CPC group compared with the control-medium group (Fig. 5A). We then evaluated the prevalence of proinflammatory (CD68⁺CD206⁻ or CD86⁺) and anti-inflammatory (CD206⁺) macrophages (M1 and M2, respectively) in the host ischemic heart 7 days after cell injection (Fig.

5B). Notably, the number of M1 macrophages (CD68⁺CD206⁻: control-CPC, 42.2 ± 25.2 per mm²; APE1-CPC, 12.0 ± 11.9 per mm²; $p < .05$; CD86⁺: control-CPC, 16.3 ± 2.4 per mm²; APE1-CPC, 9.9 ± 0.9 per mm²; $p < .05$) and the M1/M2 ratio (control-CPC, 1.46 ± 0.57 ; APE1-CPC, 0.51 ± 0.24 ; $p < .05$) were lower in mice in the APE1-CPC group compared with the control-CPC group (Fig. 5C).

Transplantation of APE1-CPCs Increased Angiogenesis and Promoted CPC Cardiomyocyte Differentiation

We examined angiogenesis in the ischemic area 7 days after cell injection. The number of CD31-positive vessels in the border zone was higher in the APE1-CPC group than in the control-medium or

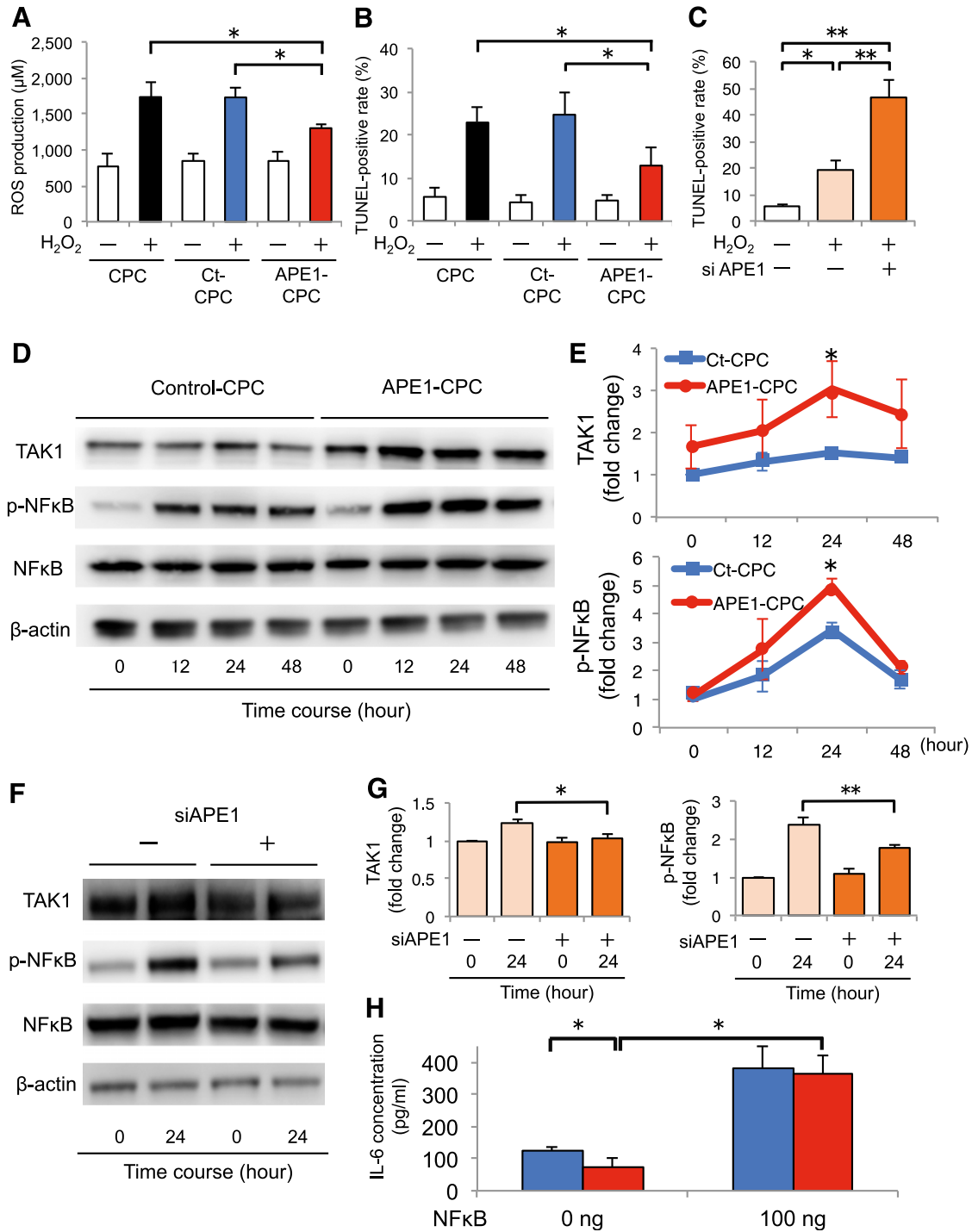


Figure 2. H₂O₂-induced ROS production and apoptosis in CPCs via activation of TAK1/NF-κB signaling. **(A):** Graph of dichloro-dihydro-fluorescein diacetate concentration (ROS production) after H₂O₂ treatment for 3 hours (*n* = 4 per group). **(B):** Number of TUNEL-positive apoptotic cells after H₂O₂ treatment for 48 hours (*n* = 6 per group). **(C):** Percentage of apoptotic CPCs transfected with siRNA against APE1 gene after H₂O₂ treatment overnight (*n* = 5, per group). **(D):** Representative blots of TAK1 and NF-κB expression in APE1-CPCs and control-CPCs upon TNF-α stimulation. **(E):** Fold change of TAK1 activation (top) and NF-κB phosphorylation (*p*-NF-κB; bottom) against baseline of control-CPCs (*n* = 7 per group). **(F):** Representative blots of TAK1 and NF-κB expression in CPCs with or without APE1 knockdown (siAPE1). **(G):** Fold change in TAK1 activation (left) and *p*-NF-κB (right) in APE1-CPCs relative to control-CPCs; after 24 hours of stimulation with TNF-α (*n* = 10 and 7 per group for TAK1 and *p*-NF-κB, respectively). **(H):** NF-κB/IL-6 ELISA assay (*n* = 5, respectively). Blue bar, control-CPC; red bar, APE1-CPC. *, *p* < .05, **, *p* < .01. Abbreviations: APE1, apurinic/apyrimidinic endonuclease/redox factor 1; CPC, cardiac progenitor cell; Ct, control; ELISA, enzyme-linked immunosorbent assay; IL, interleukin; NF, nuclear factor; ROS, reactive oxygen species; siRNA, short interfering RNA; TAK1, transforming growth factor β-activated kinase 1; TNF, tumor necrosis factor; TUNEL, terminal deoxynucleotidyl transferase dUTP nick-end labeling.

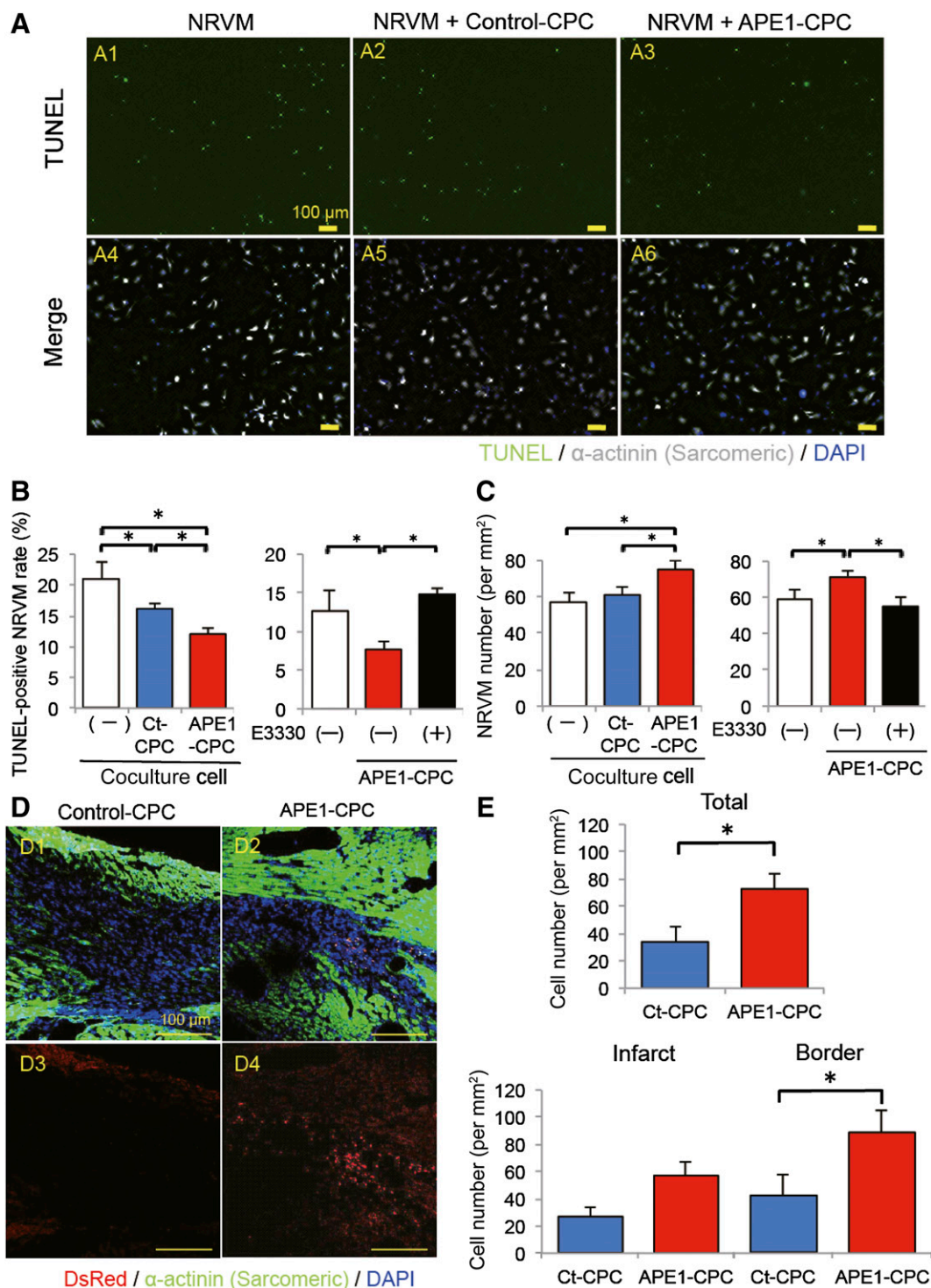


Figure 3. The mode of action of CPCs to ex vivo and in vivo ischemic heart. **(A):** Representative images of TUNEL-positive cells (green); nuclei were stained with DAPI (blue). NRVMs were labeled with an antibody against cardiac α -SA (white) (A1, A4, NRVM; A2, A5, NRVM + control-CPC; A3, A6; NRVM + APE1-CPC). Image magnification $\times 10$. **(B):** Number of TUNEL-positive apoptotic NRVMs. Significantly decreased number of apoptotic NRVMs cocultured with APE1-CPCs compared with control-CPCs ($n = 6$, NRVM; $n = 8$, NRVM + control-CPC, NRVM + APE1-CPC) and increased number of TUNEL-positive apoptotic NRVMs cocultured with APE1-CPCs by E3330 exposure ($n = 6$). Percentage of apoptotic NRVMs, as evaluated by the TUNEL assay. **(C):** Quantitative analysis of the number of NRVMs after 3 days under anoxic conditions and decreased number of NRVMs cocultured with APE1-CPCs by E3330 exposure ($n = 6$). **(D):** CPC grafts in host ischemic hearts 7 days after injection. Representative micrographs of cardiac tissue sections in control-CPC (D1, D3) and APE1-CPC (D2, D4) mice (top: merged image of transplanted cells [red], cardiac α -sarcomeric actinin [green], and cell nuclei [blue]; bottom: transplanted cells [red] and cell nuclei [blue]). Image magnification $\times 20$. **(E):** Number of DsRed-positive CPC grafts in total ischemic, infarct, and border areas of the host heart ($n = 6$ per group). *, $p < .05$. Abbreviations: APE1, apurinic/aprimidinic endonuclease/redox factor 1; CPC, cardiac progenitor cell; Ct, control; DAPI, 4',6-diamidino-2-phenylindole; NRVM, neonatal rat ventricular myocyte; SA, sarcomeric actinin; TUNEL, terminal deoxynucleotidyl transferase dUTP nick-end labeling.

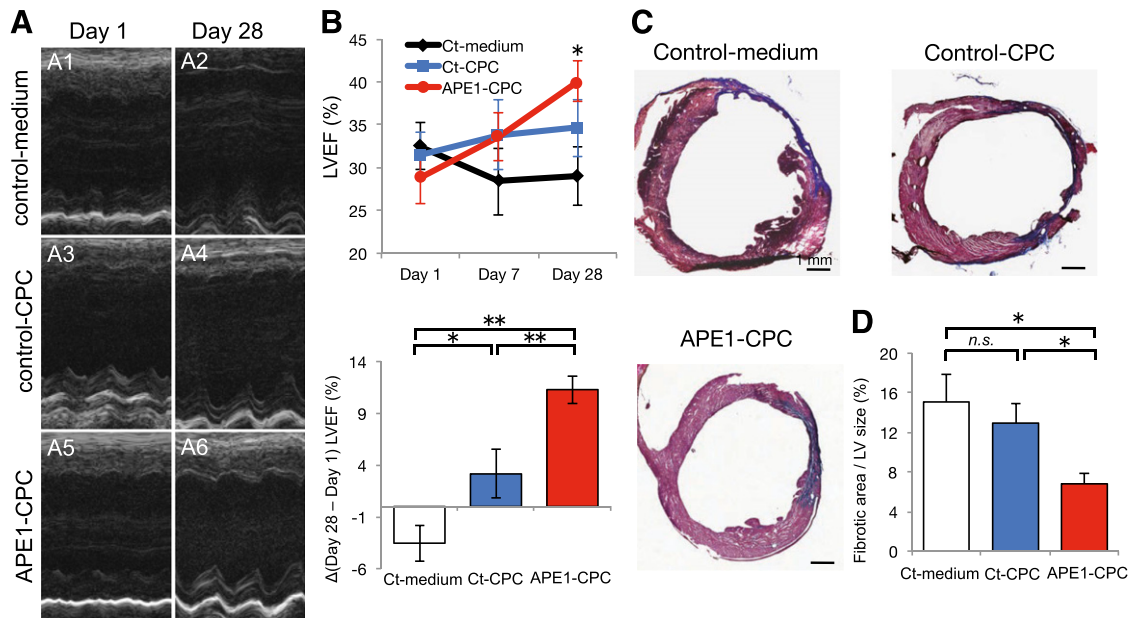


Figure 4. Cardiac function and fibrotic area by transplantation of CPCs. **(A):** Representative images of M-mode echocardiogram (short axis view) at the midlevel of the heart on days 1 (A1, A3, A5) and 28 (A2, A4, A6) post-MI. A1, A2, control-medium; A3, A4, control-CPC; A5, A6, APE1-CPC. **(B):** Absolute changes in LVEF on days 1, 7, and 28 ($n = 9$ per group) (top) (**, $p < .01$ control-medium vs. APE1-CPC at day 28) and Δ LVEF (day 28 – day 1) in three groups (bottom). **(C):** Representative images of cardiac tissue sections (short axis view) with Masson's trichrome staining on day 28 post-MI. Fibrotic areas are stained blue. **(C1):** Control-medium. **(C2):** Control-CPC. **(C3):** APE1-CPC. **(D):** Quantitative analysis of the percentage fibrotic area as a function of total LV area ($n = 9$ per group). *, $p < .05$, **, $p < .01$. Abbreviations: APE1, apurinic/aprimidinic endonuclease/redox factor 1; CPC, cardiac progenitor cell; Ct, control; LV, left ventricle; LVEF, left ventricular ejection fraction; MI, myocardial infarction; n.s., not significant.

control-CPC groups (supplemental online Fig. 3A, 3B). This finding was further confirmed by tubule formation assays with CPC conditioned medium in vitro. Notably, the tubule length of human umbilical vein endothelial cells cultured in APE1-CPC supernatant was significantly extended compared with counterparts in control-medium (supplemental online Fig. 3C, 3D). Protein analysis of CPC conditioned medium revealed significantly higher levels of vascular endothelial growth factor (VEGF) in APE1-CPC supernatant (271.1 ± 40.2 pg/ml) compared with counterparts cultured in control-CPC supernatant (72.8 ± 13.8 pg/ml; $p < .01$, $n = 6$; supplemental online Fig. 3E). Finally, we evaluated CPC differentiation in the ischemic heart of the control-CPC group and APE1-CPC group at 7 days after cell injection. The number of CPC grafts that had differentiated into cardiomyocytes (double-positive for DsRed and α -SA) was significantly higher in the APE1-CPC group (16.27 ± 6.85 cells per mm^2) than in the control-CPC group (6.86 ± 4.94 cells per mm^2 ; $p < .05$) (Fig. 6A1–A6 and 6B). After evaluating at each infarct and border zone, we found that the differentiated CPC grafts into cardiomyocytes in APE1-CPC group were significantly higher in the border zone than in the infarct zone.

DISCUSSION

Our findings demonstrated that (a) APE1 overexpression enhanced the antiapoptotic effect of CPCs under conditions of the oxidative stress via TAK1-NF- κ B pathway activation, (b) apoptosis-resistant APE1-overexpressing CPC grafts survived substantially longer in the host ischemic heart and restored LV function, and (c) successful cell grafts might provide the pleiotropic effects of the CPC grafts in host heart.

Clinical studies using various cell grafts have sought to improve the therapeutic outcome of patients with various diseases, including retinal degeneration [23], osteoarthritis [24], and myocardial infarction [25], but have shown limited success [26]. Although there are many considerations in unfavorable results, one of the most important shortcomings is the survival of graft cells in host tissue; many preclinical and clinical studies have demonstrated poor retention of cell grafts in ischemic heart [11, 27, 28]. In the severe ischemia characterized by excessive oxidative stress, cell grafts—even those comprising stem/progenitor cells—cannot survive in host organs in the absence of antiapoptotic factors. To address this limitation, a hybrid strategy combining growth factors, tissue engineering, and gene modification has been applied to cell-based therapy. We previously demonstrated that the controlled release of angiogenic cytokine (bFGF) in the host heart partially improved the survival of cardiac stem cell grafts, and that a hybrid cell therapy (cell injection with bFGF) was more effective than that of cell injection alone [12]. However, given the high technical requirements of this approach, its clinical application remains a challenge. Therefore, a simpler and more accessible strategy that incorporates gene modification is more desirable for cell-based therapy. In the present study, we showed the novel approach that APE1 overexpression enhanced the stress tolerance of cardiac progenitor cells and improved their survival in grafts transplanted into the ischemic hearts of host mice.

The APE1 enzyme has recently been characterized as a multifunctional protein that responds to various oxidative stressors to protect the organ condition, and is involved in two intrinsic pathways: (a) the BER pathway that exhibits DNA repair activity encoded at C-terminal region and (b) the redox system (Ref-1) that activates the various transcriptional factors encoded at

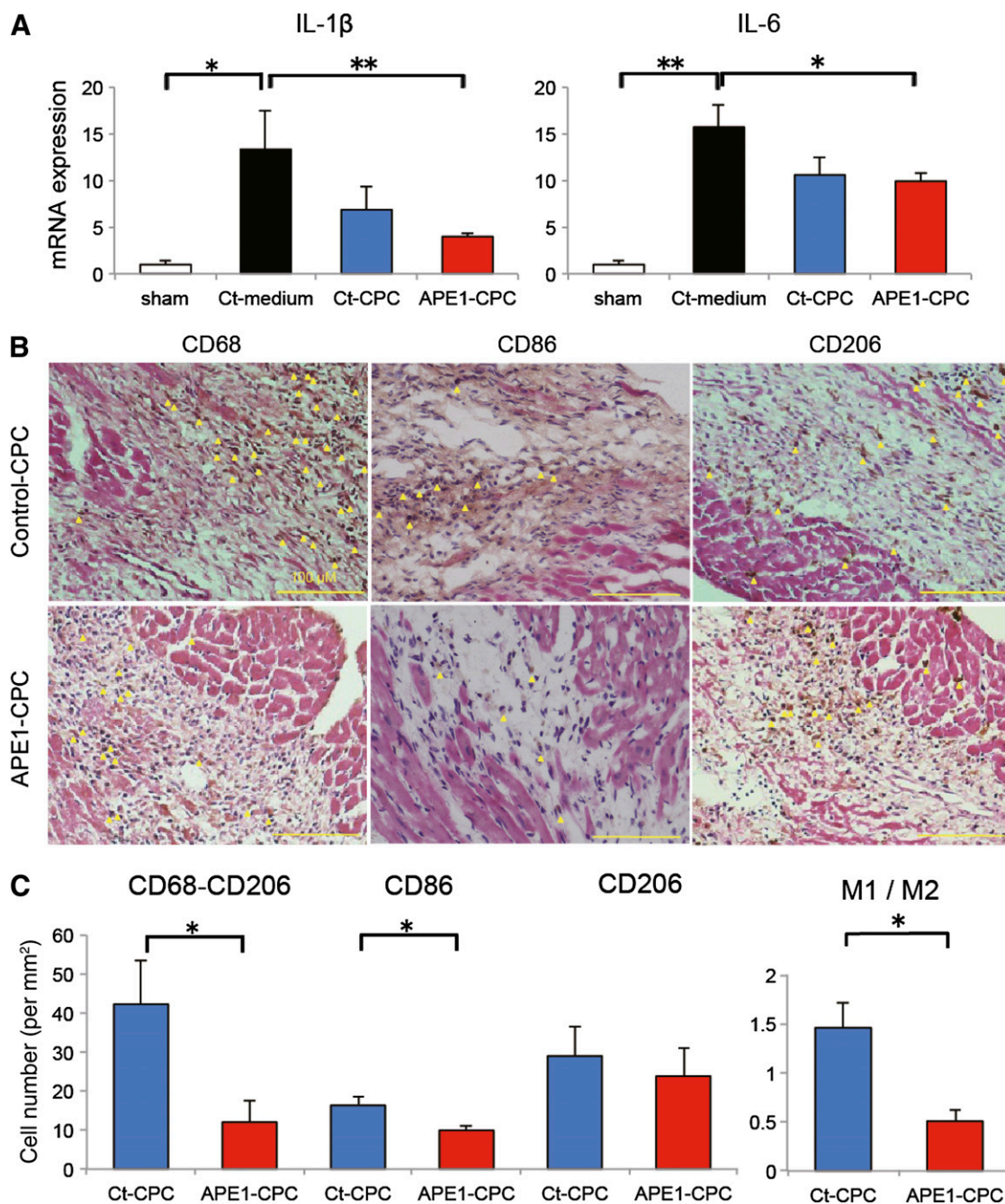


Figure 5. Cardiac inflammation attenuated by transplantation of CPCs. **(A):** Quantitative RT-PCR analysis of mRNA expression in the heart tissue of proinflammatory cytokines IL-1 β and IL-6 ($n = 5$ per group). **(B):** M1 and M2 macrophage activation in host ischemic heart 7 days post-MI. Representative cardiac tissue sections (hematoxylin and eosin staining) labeled with antibodies against CD68 (M1 and M2), CD86 (M1), and CD206 (M2) in the ischemic area. Yellow arrowheads indicate CD68-, CD86-, or CD206-positive macrophages (brown; 3,3-diaminobenzidine: DAB substrate). Scale bar, 100 μ m. **(C):** Quantitative analysis of the number of M1 (CD68⁺CD206⁻ and CD86⁺) and M2 (CD206⁺) macrophages in the ischemic area and M1/M2 ratio ($n = 6$ per group). *, $p < .05$, **, $p < .01$. Abbreviations: APE1, apurinic/apryrimidinic endonuclease/redox factor 1; CD, cluster of differentiation; CPC, cardiac progenitor cell; Ct, control; IL, interleukin; MI, myocardial infarction; RT-PCR, reverse transcription-polymerase chain reaction.

N-terminal region [13, 15, 29] and contributes to cell/tissue graft survival. In stem cell biology, BER pathway activation appears to maintain or improve “stemness” function [30, 31]. However, we found that APE1 overexpression had no effect on the expression of surface marker antigens and transcription genes (pluripotency genes *Nanog* and *Fbx15*; cardiac genes *Mef2C* and *Tert*) in undamaged CPCs. Furthermore, in immunohistochemistry analysis

of APE1 protein, intracellular localization (AP endonuclease [BER] pathway; nuclei, the redox factor; subcellular) of APE1 protein was mainly shown in subcellular portion in both normal and anoxia culture conditions. Overexpressed APE1 protein in CPCs may exert the Redox function (Ref-1) in subcellular localization without activation of AP endonuclease function. It was different from some cancer cells under oxidant stress conditions [32]. In E3330

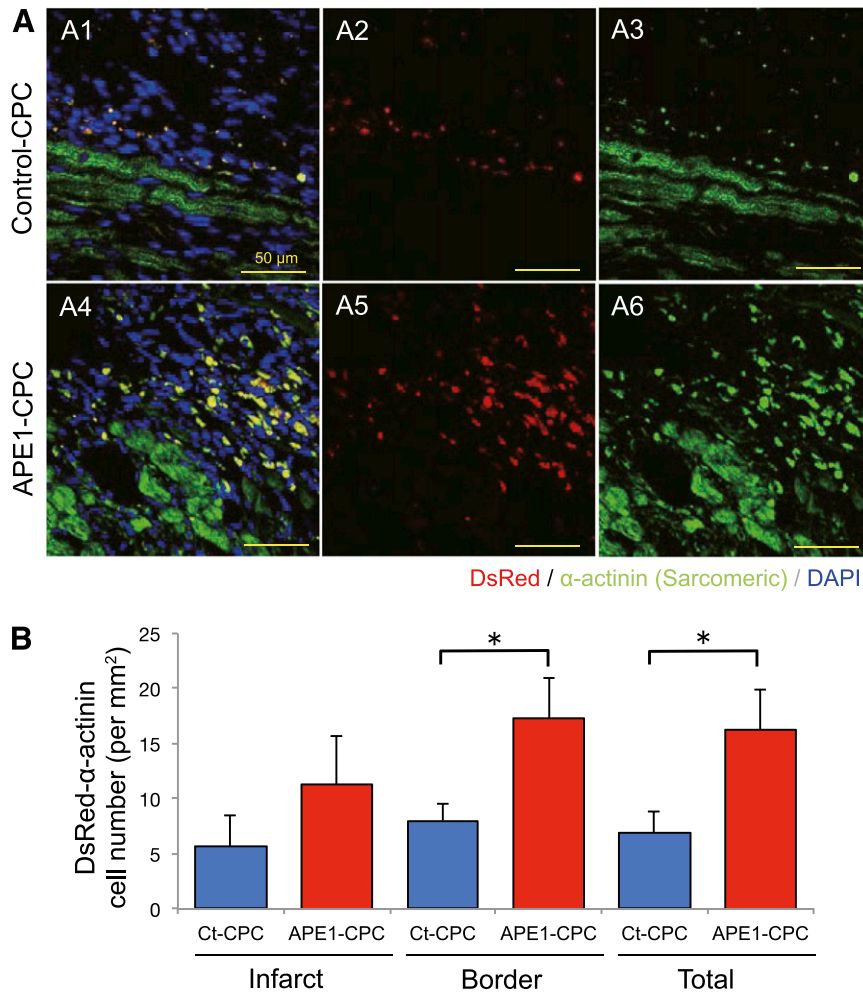


Figure 6. Cardiomyocyte differentiation of CPC grafts in host ischemic heart. **(A):** Confocal micrographs of cardiac tissue sections from control-CPC (A1–A3) and APE1-CPC (A4–A6) mice labeled for cardiac α -SA expression on day 7 after injection. Middle: transplanted cells (red); right: cardiac α -SA (green); left: merged image of transplanted cells (red), cardiac α -SA (green), and cell nuclei stained with DAPI (blue). **(B):** Number of CPC grafts positive for cardiac α -SA in the total ischemic area and border and infarct areas. **(C):** Ratio of cardiac α -SA-positive CPC grafts in each area ($n = 6$ per group). Scale bar, 50 μ m. *, $p < .05$. Abbreviations: APE1, apurinic/apryrimidinic endonuclease/redox factor 1; CPC, cardiac progenitor cell; Ct, control; DAPI, 4',6-diamidino-2-phenylindole; SA, sarcomeric actinin.

assay, the inhibitory effect of APE1 overexpression against anoxia-induced apoptosis was canceled by E3330 exposure. Thus, we think that the role of the redox function (Ref-1) of APE1 is strongly associated with antiapoptotic effects against oxidant stress, which are mediated by transcription factors such as activator protein 1, hypoxia-inducible factor-1 α [16], and NF- κ B. APE1-overexpressing CPC grafts survived under ischemic conditions owing to the antiapoptotic function of APE1. NF- κ B is a primary factor known to confer protection against oxidative stress [33, 34] and is also known as a pleiotropic transcription factor, which acts as an antiapoptotic transcriptional regulator or inflammatory stimulator under several stress conditions. During protein array analysis of enzyme regulation in APE1-overexpressing CPCs during oxidative stress, we found that TAK1—a component of the NF- κ B pathway that inhibits apoptotic cell death stimulated by TNF- α [35]—was upregulated in APE1-CPCs compared with controls. Furthermore, TNF- α induced an increase in TAK1 expression, and consequently NF- κ B phosphorylation, in APE1-CPCs, which was attenuated by the knockdown of APE1. Hence, in our experimental conditions in which APE1 overexpression

provided the antiapoptotic effect, we suggested that NF- κ B would be crucial in the protective effect of CPCs. Our results first demonstrated that APE1 regulates TAK1 and exerts an antiapoptotic effect in cell grafts via transcriptional activation of NF- κ B. Thus, the APE1-dependent redox response may potentially improve the efficacy of cardiac cell therapy, in part via TAK1-NF- κ B pathway activation.

CPCs are tissue-specific somatic stem cells that adopt a cardiac fate [36, 37], although they exhibit a variety of phenotypes. Sca-1-positive CPCs have great promise for cardiac cell therapy because of their higher potential for differentiating into cells that express cardiac markers—including transcription factors and tissue-specific proteins such as a cardiac α -SA—compared with other somatic stem cell types, and they show spontaneous beating [38, 39]. In the present study, we also showed that Sca-1-positive CPCs differentiated into mature cardiomyocytes expressing cardiac α -SA with a sarcomeric structure in an NRVM coculture system, and the transplantation of control-CPCs improved the LVEF of MI heart as in previous reports [38, 39]. Moreover, despite the fact that CPC cardiogenesis was unaffected by APE1 overexpression,

many CPC grafts survived by APE1 overexpression differentiated into cardiomyocytes in the ischemic host heart and restored cardiac function more dramatically than control-CPC grafts. APE1-mediated CPC graft survival may therefore maximize their cardiac differentiation potential. Furthermore, the superior angiogenic effects observed in APE1-CPC transplants may be the result of the excess VEGF secretion also identified in this study.

Meanwhile, keeping the structure and function of the infarcted heart involves several factors [1]. We found that APE1 overexpression increased the anti-inflammatory effects of CPCs, as lower proinflammatory cytokine (IL-1 β and IL-6) expression and M1 macrophage accumulation was observed. Several reports have previously shown that mesenchymal stem cell transplantation conveys anti-inflammatory effects to host damaged organs, as seen with models of graft-versus-host disease [40] and MI [41, 42]. Accordingly, Sca-1-positive CPCs also exerted anti-inflammatory effects to damaged host heart because they have a phenotype (CD106 and CD29) similar to mesenchymal stem cells. In addition, improving the survival of APE1-overexpressing CPCs could further attenuate cardiac inflammation after myocardial infarction and might provide the antiapoptotic effect to host cardiomyocytes, such as decreasing NRVM apoptosis in ex vivo coculture experiments. Taken together, these findings highlight the pleiotropic actions of the transplanted APE1-overexpressing CPCs that exhibit both cardiac regeneration and angiogenesis functions in a protective capacity by exerting anti-inflammatory and antiapoptotic effects of the host heart. This strategy may serve as a novel approach to cardiac cell therapy.

A limitation of this study is that the endonuclease site (the BER pathway) was not activated in undamaged APE1-CPCs. We speculate that APE1 gene overexpression did not affect the CPC phenotype in normal conditions because of its high potential as a stem/progenitor cell. Another limitation of this study is that it did not address whether APE1 enzyme contributed directly to the repair of the ischemic heart. In the preliminary studies, we confirmed the increased expression of APE1 gene in the mouse heart 5 days after myocardial infarction (data not shown); however, this was a transient response to stress stimuli that did not persist after the acute phase. Given that the repair of the host heart via pleiotropic effects induced by cell-based therapy occurs not only during the acute phase but also during the chronic phase, the effects of APE1 enzyme may be limited in the infarcted heart. A final limitation of our study is the timing of cell injections into

mouse hearts. Varied injection times should be used postischemia to fully evaluate the therapeutic potential of CPCs; however, reoperative mouse death was a noted concern with CPC injection 3–5 days after myocardial infarction in the MI mouse model. To clarify differences in APE1-CPC and control-CPC grafting, it was important that APE1-CPCs could survive more than control-CPCs for at least 7 days after myocardial ischemia. We plan to use larger animals in future preclinical analyses on the effects of APE1-CPC transplantation after disease establishment.

CONCLUSION

APE1 hindered apoptosis in CPC grafts subjected to oxidative stress in part because of increased TAK1-NF- κ B pathway activation. Furthermore, APE1-CPC grafts that effectively survived in the ischemic heart restored cardiac function and attenuated myocardial infarct size through pleiotropic mechanisms that remain to be characterized. These findings suggest that APE1 gene overexpression in CPCs may be a novel strategy to reinforce cardiac cell therapy.

ACKNOWLEDGMENTS

We thank Kaori Kanno and Yuki Taira for help with data collection and for providing helpful suggestions during this study and Yasuaki Saijo (Division of Community Medicine and Epidemiology, Department of Health Science, Asahikawa Medical University) for help with statistical data analysis. This work was supported by Grants-in-Aid from the Ministry of Education, Culture, Sports, Science, and Technology of Japan.

AUTHOR CONTRIBUTIONS

T.A.: conception and design, data analysis and interpretation, manuscript writing; N.T.: conception and design, data analysis and interpretation, manuscript writing, final approval of manuscript; K.M., M.K., M.M., A.Y., and J.K.: data analysis and interpretation; N.H.: final approval of manuscript.

DISCLOSURES

The authors indicated no potential conflicts of interest.

REFERENCES

- Malliaras K, Marbán E. Cardiac cell therapy: where we've been, where we are, and where we should be headed. *Br Med Bull* 2011;98:161–185.
- Assmus B, Honold J, Schächinger V et al. Transcatheter transplantation of progenitor cells after myocardial infarction. *N Engl J Med* 2006;355:1222–1232.
- Stamm C, Kleine HD, Choi YH et al. Intramyocardial delivery of CD133+ bone marrow cells and coronary artery bypass grafting for chronic ischemic heart disease: Safety and efficacy studies. *J Thorac Cardiovasc Surg* 2007;133:717–725.
- Losordo DW, Henry TD, Davidson C et al; ACT34-CMI Investigators. Intramyocardial, autologous CD34+ cell therapy for refractory angina. *Circ Res* 2011;109:428–436.
- Menasché P, Alfieri O, Janssens S et al. The Myoblast Autologous Grafting in Ischemic Cardiomyopathy (MAGIC) trial: First randomized placebo-controlled study of myoblast transplantation. *Circulation* 2008;117:1189–1200.
- Trachtenberg B, Velazquez DL, Williams AR et al. Rationale and design of the Transendocardial Injection of Autologous Human Cells (bone marrow or mesenchymal) in Chronic Ischemic Left Ventricular Dysfunction and Heart Failure Secondary to Myocardial Infarction (TAC-HFT) trial: A randomized, double-blind, placebo-controlled study of safety and efficacy. *Am Heart J* 2011; 161:487–493.
- Rosenzweig A. Cardiac cell therapy—mixed results from mixed cells. *N Engl J Med* 2006;355: 1274–1277.
- Bolli R, Chugh AR, D'Amario D et al. Cardiac stem cells in patients with ischaemic cardiomyopathy (SCIPIO): Initial results of a randomised phase 1 trial. *Lancet* 2011; 378:1847–1857.
- Makkar RR, Smith RR, Cheng K et al. Intracoronary cardiosphere-derived cells for heart regeneration after myocardial infarction (CADUCEUS): A prospective, randomised phase 1 trial. *Lancet* 2012;379:895–904.
- Penicka M, Widimsky P, Kobyłka P et al. Images in cardiovascular medicine. Early tissue distribution of bone marrow mononuclear cells after transcatheter transplantation in a patient with acute myocardial infarction. *Circulation* 2005;112:e63–e65.
- Amsalem Y, Mardor Y, Feinberg MS et al. Iron-oxide labeling and outcome of transplanted mesenchymal stem cells in the infarcted myocardium. *Circulation* 2007;116(suppl):I38–I45.

- 12** Takehara N, Tsutsumi Y, Tateishi K et al. Controlled delivery of basic fibroblast growth factor promotes human cardiosphere-derived cell engraftment to enhance cardiac repair for chronic myocardial infarction. *J Am Coll Cardiol* 2008;52:1858–1865.
- 13** Bhakat KK, Mantha AK, Mitra S. Transcriptional regulatory functions of mammalian AP-endonuclease (APE1/Ref-1), an essential multifunctional protein. *Antioxid Redox Signal* 2009;11:621–638.
- 14** Thakur S, Sarkar B, Cholia RP et al. APE1/Ref-1 as an emerging therapeutic target for various human diseases: Phytochemical modulation of its functions. *Exp Mol Med* 2014;46:e106.
- 15** Xanthoudakis S, Miao GG, Curran T. The redox and DNA-repair activities of Ref-1 are encoded by nonoverlapping domains. *Proc Natl Acad Sci USA* 1994;91:23–27.
- 16** Ema M, Hirota K, Mimura J et al. Molecular mechanisms of transcription activation by HLF and HIF1alpha in response to hypoxia: Their stabilization and redox signal-induced interaction with CBP/p300. *EMBO J* 1999;18:1905–1914.
- 17** Gaiddon C, Moorthy NC, Prives C. Ref-1 regulates the transactivation and pro-apoptotic functions of p53 in vivo. *EMBO J* 1999;18:5609–5621.
- 18** Guan Z, Basu D, Li Q et al. Loss of redox factor 1 decreases NF-kappaB activity and increases susceptibility of endothelial cells to apoptosis. *Arterioscler Thromb Vasc Biol* 2005;25:96–101.
- 19** Herring CJ, West CM, Wilks DP et al. Levels of the DNA repair enzyme human apurinic/aprimidinic endonuclease (APE1, APEX, Ref-1) are associated with the intrinsic radiosensitivity of cervical cancers. *Br J Cancer* 1998;78:1128–1133.
- 20** Martinet W, Knaapen MW, De Meyer GR et al. Elevated levels of oxidative DNA damage and DNA repair enzymes in human atherosclerotic plaques. *Circulation* 2002;106:927–932.
- 21** Stetler RA, Gao Y, Zukin RS et al. Apurinic/aprimidinic endonuclease APE1 is required for PACAP-induced neuroprotection against global cerebral ischemia. *Proc Natl Acad Sci USA* 2010;107:3204–3209.
- 22** Yamauchi A, Kawabe J, Kabara M et al. Apurinic/aprimidinic endonuclease 1 maintains adhesion of endothelial progenitor cells and reduces neointima formation. *Am J Physiol Heart Circ Physiol* 2013;305:H1158–H1167.
- 23** Schwartz SD, Regillo CD, Lam BL et al. Human embryonic stem cell-derived retinal pigment epithelium in patients with age-related macular degeneration and Stargardt's macular dystrophy: Follow-up of two open-label phase 1/2 studies. *Lancet* 2015;385:509–516.
- 24** Jo CH, Lee YG, Shin WH et al. Intra-articular injection of mesenchymal stem cells for the treatment of osteoarthritis of the knee: A proof-of-concept clinical trial. *STEM CELLS* 2014;32:1254–1266.
- 25** Tongers J, Losordo DW, Landmesser U. Stem and progenitor cell-based therapy in ischemic heart disease: Promise, uncertainties, and challenges. *Eur Heart J* 2011;32:1197–1206.
- 26** Gyöngyösi M, Wojakowski W, Lemarchand P et al; ACCRUE Investigators. Meta-Analysis of Cell-based CaRdiac stUdiEs (ACCRUE) in patients with acute myocardial infarction based on individual patient data. *Circ Res* 2015;116:1346–1360.
- 27** Müller-Ehmsen J, Krausgrill B, Burst V et al. Effective engraftment but poor mid-term persistence of mononuclear and mesenchymal bone marrow cells in acute and chronic rat myocardial infarction. *J Mol Cell Cardiol* 2006;41:876–884.
- 28** Freyman T, Polin G, Osman H et al. A quantitative, randomized study evaluating three methods of mesenchymal stem cell delivery following myocardial infarction. *Eur Heart J* 2006;27:1114–1122.
- 29** Barzilay G, Hickson ID. Structure and function of apurinic/aprimidinic endonucleases. *BioEssays* 1995;17:713–719.
- 30** Domenis R, Bergamin N, Gianfranceschi G et al. The redox function of APE1 is involved in the differentiation process of stem cells toward a neuronal cell fate. *PLoS One* 2014;9:e89232.
- 31** Gurusamy N, Mukherjee S, Lekli I et al. Inhibition of ref-1 stimulates the production of reactive oxygen species and induces differentiation in adult cardiac stem cells. *Antioxid Redox Signal* 2009;11:589–600.
- 32** Tell G, Fantini D, Quadrigoglio F. Understanding different functions of mammalian AP endonuclease (APE1) as a promising tool for cancer treatment. *Cell Mol Life Sci* 2010;67:3589–3608.
- 33** Beg AA, Baltimore D. An essential role for NF-kappaB in preventing TNF-alpha-induced cell death. *Science* 1996;274:782–784.
- 34** Vasko MR, Guo C, Kelley MR. The multifunctional DNA repair/redox enzyme Ape1/Ref-1 promotes survival of neurons after oxidative stress. *DNA Repair (Amst)* 2005;4:367–379.
- 35** Omori E, Matsumoto K, Sanjo H et al. TAK1 is a master regulator of epidermal homeostasis involving skin inflammation and apoptosis. *J Biol Chem* 2006;281:19610–19617.
- 36** Oh H, Bradfute SB, Gallardo TD et al. Cardiac progenitor cells from adult myocardium: Homing, differentiation, and fusion after infarction. *Proc Natl Acad Sci USA* 2003;100:12313–12318.
- 37** Messina E, De Angelis L, Frati G et al. Isolation and expansion of adult cardiac stem cells from human and murine heart. *Circ Res* 2004;95:911–921.
- 38** Matsuura K, Nagai T, Nishigaki N et al. Adult cardiac Sca-1-positive cells differentiate into beating cardiomyocytes. *J Biol Chem* 2004;279:11384–11391.
- 39** Tateishi K, Ashihara E, Takehara N et al. Clonally amplified cardiac stem cells are regulated by Sca-1 signaling for efficient cardiovascular regeneration. *J Cell Sci* 2007;120:1791–1800.
- 40** Le Blanc K, Frassoni F, Ball L et al. Mesenchymal stem cells for treatment of steroid-resistant, severe, acute graft-versus-host disease: A phase II study. *Lancet* 2008;371:1579–1586.
- 41** van den Akker F, Deddens JC, Doevendans PA et al. Cardiac stem cell therapy to modulate inflammation upon myocardial infarction. *Biochim Biophys Acta* 2013;1830:2449–2458.
- 42** Cho DI, Kim MR, Jeong HY et al. Mesenchymal stem cells reciprocally regulate the M1/M2 balance in mouse bone marrow-derived macrophages. *Exp Mol Med* 2014;46:e70.



See www.StemCellsTM.com for supporting information available online.